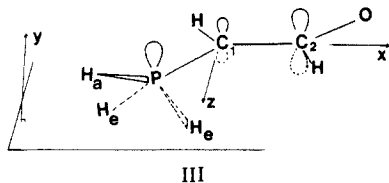


**Table I.** ESR Tensors (MHz) Measured for Signals A and Calculated Couplings for [H<sub>3</sub>PCHC(O)H]<sup>••</sup>

tensor	eigenvalues	eigenvectors <sup>a</sup>	anisotropic couplings	spin densities	calcd couplings <sup>c</sup>
$\bar{g}$	2.0023 2.0051 2.0065	0.035, -0.9612, 0.2736 0.3810, +0.2659, 0.8855 -0.9239, +0.0733, 0.3755			
<sup>31</sup> P- $\bar{T}$	(+) <sup>879</sup> (+) <sup>538</sup> (+) <sup>546</sup>	-0.3346, -0.7923, 0.5102	$\tau_1 = (+)225$ $\tau_2 = (-)116$ $\tau_3 = (-)108$	$\rho_p = 0.30$	$\tau_1' = 167$ $\tau_2' = -92$ $\tau_3' = -74$
<sup>1</sup> H- $\bar{T}$	$A_{iso} = (+)654$ (-) <sup>4</sup> (-) <sup>22</sup> (-) <sup>35</sup> $A_{iso} = (-)20.3$	0.7684, 0.2557, 0.5867 -0.1582, -0.8124, 0.5613 -0.6201, 0.5241, 0.5838	$\tau_1 = (+)16.3$ $\tau_2 = (-)1.7$ $\tau_3 = (-)14.7$	$\rho_s = 0.045$  $\rho_c = 0.31^b$	$A_{iso} = 225$ $\tau_1' = 11.4$ $\tau_2' = -3.0$ $\tau_3' = -8.4$ $A_{iso} = -16.5$

<sup>a</sup> ESR reference frame:  $-0x//c, -0y//b, -0z//a^*$ . <sup>b</sup> Estimated spin density on the carbon bound to the proton. <sup>c</sup> Hyperfine couplings calculated for structure III.

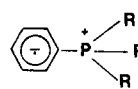
constant [ $\rho_c = A_{iso}/A(^*CH_3) = 0.31$ ]. The orientation of the phosphorus p orbital which participates in the SOMO is given by the eigenvector associated with the maximum phosphorus anisotropic coupling, <sup>31</sup>P- $\bar{T}_{max}$ . This direction is found to be rather close to that of the radical carbon p<sub>x</sub> orbital since the angle (<sup>1</sup>H- $\bar{T}_2$ , <sup>31</sup>P- $\bar{T}_{max}$ ) is equal to only 10°. These properties agree with those expected for a (R<sub>3</sub>P=C(H)=C(O)H)<sup>•</sup> radical, but the  $\pi$  direction does not coincide with the direction perpendicular to the CCP plane in the crystal. We have therefore used ab initio calculations<sup>14,15</sup> in order to get information about the spin densities and hyperfine coupling tensors for some selected geometries of (H<sub>3</sub>PCHC(O)H)<sup>••</sup>. We could not find any acceptable agreement between experimental and calculated results when the tetrahedral coordination of the phosphorus, observed in the crystal structure, was maintained. A good accord was found, however, by imposing a trigonal-bipyramidal structure on the phosphoranyl moiety (structure III):  $\angle C(1)PH_a = 150^\circ$ ,  $\angle C(1)PH_c = 100^\circ$ , and  $\angle PC(1)C(2) = 119^\circ$ .



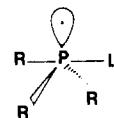
The calculated spin densities and hyperfine tensors are very sensitive to the P-C and C-C lengths; we give, in Table I, the coupling parameters calculated for C(1)-C(2) = 1.48 Å, P-C(1) = 1.7 Å, and C-O = 1.46 Å. The unpaired electron is mainly delocalized in atomic p<sub>y</sub> orbitals [ $\rho_y(P) = 0.36$ ,  $\rho_y(C1) = -0.10$ ,  $\rho_y(C2) = 0.26$ ,  $\rho_y(O) = 0.12$ ] and in a phosphorus s orbital [ $\rho_s(P) = 0.07$ ]. A small spin density ( $\rho_z = 0.09$ ) is also found in the phosphorus p<sub>z</sub> orbital. The calculated tensors lead to a (<sup>31</sup>P- $\bar{T}_{||}$ , <sup>1</sup>H- $\bar{T}_2$ ) angle equal to 14°. The small negative spin density on the central carbon explains why a second <sup>1</sup>H coupling is not observed on the ESR spectrum (line width ~ 4 G), and the reorganization of the ligands around the phosphorus atom is certainly the cause of the reorientation of the normal to the PCC plane.

The role of the R' group in the stabilization of the allylic structure, (R<sub>3</sub>P=C(H)=C(H)R')<sup>•</sup>, lies therefore in its ability to destabilize a phosphonium moiety. When R' is an electrodonor group, it makes more difficult the transfer of an electron from the phosphorus toward the ethylenic system [which would yield the analogue of the previously reported structure IVa for the phosphoranyl radical (C<sub>6</sub>H<sub>5</sub>)PR<sub>3</sub><sup>16</sup>] and so allows conjugation of

the equatorial phosphoranyl orbital (TBP structure, IVb) with the  $\pi$  system of the olefin moiety L.<sup>17</sup>



IVa



IVb

**Acknowledgment.** We thank the Swiss National Research Fund for their support.

**Supplementary Material Available:** ESR spectrum and angular variation of the signals and a listing of crystallographic data including atomic coordinates and bond lengths and angles for Ph<sub>3</sub>P=C(H)=C(O)H (8 pages). Ordering information is given on any current masthead page.

(16) (a) Boeckstein, G.; Jansen, E. H. J. M.; Buck, H. M. J. *Chem. Soc., Chem. Commun.* **1974**, 118. (b) Davies, A. G.; Parrot, M. J.; Roberts, B. P. *J. Chem. Soc., Chem. Commun.* **1974**, 973. (c) Janssen, R. A. J.; Visser, G. J.; Buck, H. M. J. *Am. Chem. Soc.* **1984**, *106*, 3429.

(17) Studies are underway to detect other delocalized radicals derived from phosphoranes and to optimize the structure of some phosphoallyl radicals.

### Cloth-like Aggregates of Micellar Fibers Made of N-Dodecyltartaric Acid Monoamides

Jürgen-Hinrich Fuhrhop,\* Corinna Demoulin,  
Jörg Rosenberg, and Christoph Boettcher

*Institut für Organische Chemie  
Freien Universität Berlin  
Takustrasse 3, 1000 Berlin 33, West Germany*

*Received October 17, 1989*

Amphiphiles with an electroneutral glyconamide head group and N-alkyl chains ranging from C-7 to C-12 form micellar fibers of bimolecular thickness in aqueous solution that are stabilized by amide hydrogen-bond chains.<sup>1</sup> At elevated temperatures and/or in the presence of detergents, such fibers are long-lived,<sup>2</sup> but at room temperature, the pure amphiphiles usually precipitate within a few hours. From anionic polymer fibers it is known that the repulsive interaction of negatively charged surfaces, e.g., in tobacco mosaic virus (TMV),<sup>3,4</sup> keeps fibers apart from each other. We therefore investigated several chiral and anionic amphiphiles, for example, the tartaric amide monocarboxylates **1a,b**,<sup>5</sup> for their

(14) (a) Binkley, J. G.; Whiteside, R. A.; Krishnan, R.; Seeger, R.; DeFrees, D. J.; Schlegel, H. B.; Topiol, S.; Kahn, L. R. *QCP* **1981**, *13*, 406. (b) Binkley, J. S.; Frisch, M. J.; DeFrees, D. J.; Raghavachari, K.; Whiteside, R. A.; Schlegel, H. B.; Fluder, E. M.; Pople, J. A. *GAUSSIAN 82*; Carnegie-Mellon University: Pittsburgh, PA, 1982.

(15) UHF calculations have been performed by using a 6-31G\* basis set. The spin densities have been calculated after spin annihilation of the quartet contamination. (Cremaschi, P.; Gamba, A.; Morosi, G.; Simonetta, M. *Theor. Chim. Acta* **1976**, *41*, 177.) The final value of  $\langle S^2 \rangle = 0.753$ . For details about the calculation of the hyperfine tensors, see ref 5.

(1) Fuhrhop, J.-H.; Schnieder, P.; Rosenberg, J.; Boekema, E. *J. Am. Chem. Soc.* **1987**, *109*, 3387-3390.

(2) Fuhrhop, J.-H.; Svenson, S.; Boettcher, C.; Vieth, H. M.; Roessler, E. *J. Am. Chem. Soc.* In press.

(3) Millman, B. M.; Nickel, B. G. *Biophys. J.* **1980**, *32*, 49-63.

(4) Podgornik, R.; Rau, D. C.; Parsegian, V. A. *Macromolecules* **1989**, *22*, 1780-1786.

(5) Prepared from di-O-acetyltartaric anhydrides and dodecylamine by conventional methods.

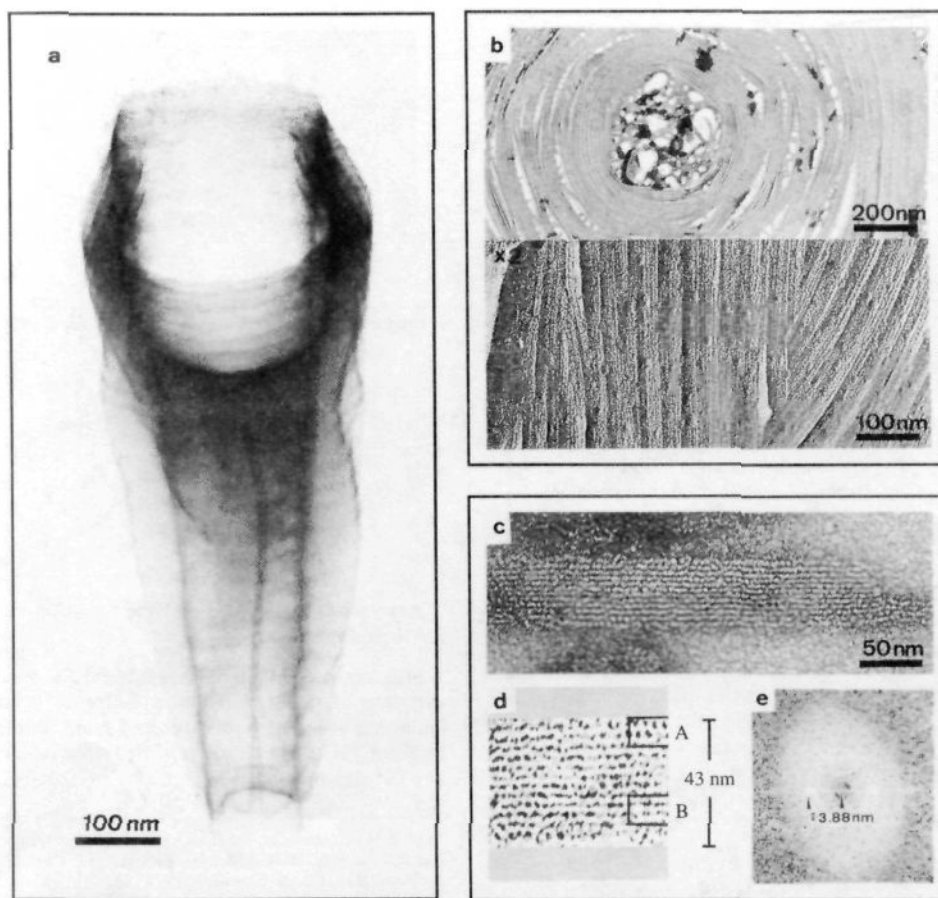
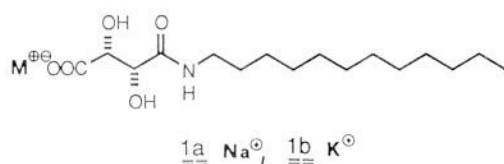


**Figure 1.** A typical, multilayered cloth made of potassium tartaric amide **1b** at pH 5. Its observed physical shape is fortuitous.<sup>5</sup> (Negative stain, uranyl acetate 1%.) (b) Freeze-etching of a similar multilayer made of the sodium salt **1a**.<sup>5</sup> At higher magnification (below), the bilayer profiles become visible (Pt/C shadowed). (c) Fiber pattern of **1a**. (Negative stain, uranyl acetate 1%.) (d) Digitized area of the fiber bundle taken from Figure 1c. (e) Fourier transform of the input image from Figure 1d, as obtained by calculating the reciprocal space frequencies ( $x$ - $y$  exchanged). Two intense spots yield a periodical pattern of 38.78 Å.

ability to produce long-lived micellar fibers that resist crystallization.



We could indeed produce stable gels containing long-lived fibers of the ultimate thinness of a molecular bilayer (39 Å) from both the sodium and potassium salts by lowering the pH of hot micellar solutions to 4.1–4.9 and cooling the solutions down to room temperature. The same procedure at pH > 5 led to crystal formation, whereas below pH 4 ill-defined precipitates were observed. Since the critical pH is close to the  $pK_a$  of tartaric acid, we assume that about half of its carboxyl groups are protonated in the fibers. Tight packing of the molecules within the micellar rod leads to about 18 molecules within one micellar turn or about 50 molecules in a rod segment of 10-Å length.<sup>6</sup> The resulting charge density<sup>6</sup> of roughly 20–30 e/nm of rod length is approximately the same as the assumed density of 35 e/nm in TMV.<sup>3</sup>

To our surprise, the anionic micellar rods, however, did not separate. They rather aggregated to form unique cloth-like multilayers of micellar fibers (Figure 1a). The potassium salts

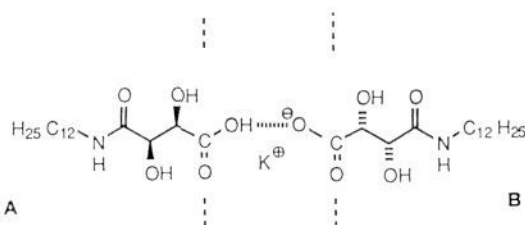


**Figure 2.** Hydrogen bonding between two neighboring, partly protonated micellar fibers A and B.

produced aggregates of micrometer dimensions that were easily observable by light microscopy, as well as on electron micrographs, whereas the sodium salt tended to give smaller, more tightly ordered aggregates.<sup>7</sup> Determination of the diameters of the threads by measuring extended cloth areas and dividing by the number of threads invariably leads to the dimensions of a molecular bilayer for one thread ( $36 \pm 3$  Å). This means that the single fibers are tightly linked to each other and there is no intermediate space. Image processing of a large area of the fibers (Figure 1b) originating from the sodium salt **1a** also showed a periodicity in the  $x$  axis (Figure 1c) of  $39 \pm 1$  Å, obtained by Fourier transform (Figure 1e) of the digitized area in Figure 1d. The irregular periodicity in the  $y$  axis, which is apparently also present, could not be resolved because small regions with well-

(6) Based on the fiber model given by Fuhrhop et al. (Figure 8: Fuhrhop, J.-H.; Schnieder, P.; Boekema, E.; Helfrich, W. *J. Am. Chem. Soc.* **1988**, *110*, 2861–2867) and the assumption of one charge per amphiphilic molecule.

(7) More electron micrographs are provided in the supplementary material. Structures of the sheets and threads were independent of staining methods. Micrographs of freeze-etched samples showed identical structures.

ordered, separated threads (e.g., B in Figure 1d) are followed by irregular regions with partial fusions of the threads (e.g., A in Figure 1d).

The primary molecular binding forces between two threads are presumably hydrogen-bond chains between carboxyl protons and carboxylate anions of neighboring fibers (Figure 2). A similar situation has been encountered in crystals of tartaric acid salts: they are most stable if hydrogen-bonded water molecules and counterions ( $H^+$ ,  $NH_4^+$ ) are bound together with one alkali-metal ion.<sup>8,9</sup> Pasteur's sodium ammonium tartrate hydrate being the most famous example.<sup>8</sup>

Separated threads or sheets of bilayers have also been observed in cubic and hexagonal phases,<sup>10</sup> myelin figures,<sup>11,12</sup> or multiwalled vesicles<sup>12</sup> consisting of double-chain amphiphiles in aqueous emulsions. None of these materials form complex shapes and isolated bodies such as shown in Figure 1a. It is presumably the relatively good water solubility of the amphiphiles **1a,b** in micellar form that allows rapid interfiber associations.<sup>2</sup>

As usual with ultrathin micellar fibers, only the pure enantiomers of **1a,b** produce such aggregates with large surfaces. The corresponding racemate rather forms smooth planar bilayer platelets under the same conditions<sup>7</sup> and precipitates from aqueous solution ("chiral bilayer effect"<sup>1</sup>).

**Acknowledgment.** We thank Prof. E. Zeitler for his continuous interest and P. Dube for kind help with image processing. This work was supported by the Deutsche Forschungsgemeinschaft (SFB 312 "Vectorial Membrane Processes"), the FNK of the Freie Universität Berlin, and the Fonds der Chemischen Industrie.

**Supplementary Material Available:** Electron micrographs of different cloth structures made of micellar fiber aggregates of potassium salt **1b** and sodium salt **1a** (6 pages). Ordering information is given on any current masthead page.

(8) Kuroda, R.; Mason, S. F. *J. Chem. Soc., Dalton Trans.* **1981**, 1268–1273.

(9) Pasteur, L. C. R. *Hebd. Seances Acad. Sci.* **1848**, 26, 535.

(10) Lindblom, G.; Rilfors, L. *Biochim. Biophys. Acta* **1989**, *988*, 221–256 and references therein.

(11) Sakurai, I.; Kawamura, Y.; Sakurai, T.; Idegami, A.; Seto, T. *Mol. Cryst. Liq. Cryst.* **1985**, *130*, 203–222.

(12) Murakami, Y.; Nakano, A.; Yoshimatsu, A.; Uchitomi, K.; Matsuda, Y. *J. Am. Chem. Soc.* **1984**, *106*, 3613–3623.

## Polymerized Liposomes Designed To Probe and Exploit Ligand-Receptor Recognition at the Supramolecular Level<sup>1</sup>

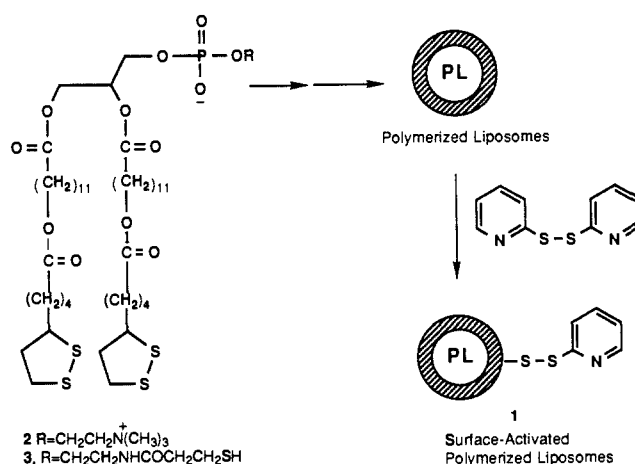
Nancy Dodrer<sup>2</sup> and Steven L. Regen\*

Department of Chemistry and  
Zettlemoyer Center for Surface Studies  
Lehigh University, Bethlehem, Pennsylvania 18015

Received December 20, 1989

This paper describes the synthesis of surface-activated polymerized liposomes (**1**) derived from 1,2-bis[12-(lipoyloxy)dodecanoyl]-*sn*-glycero-3-phosphocholine (**2**) and 1,2-bis[12-(lipoyloxy)dodecanoyl]-*sn*-glycero-3-phospho-*N*-(3-mercaptopropionyl)ethanolamine (**3**). Such liposomes, which bear activated sites that are locked into a random distribution on the membrane surface, have a surface density that can be controlled by adjusting the molar ratio of **2/3** that is used, and reversibly bind organic thiols, should provide a unique opportunity for probing and exploiting ligand-receptor recognition at the supramolecular level.

Understanding how biological membranes recognize and respond to extracellular signals, and learning how to control such



recognition, represent two of the most important challenges presently facing chemists and biologists. At the supramolecular level, the key issues extend beyond the specific chemistries involved; they relate to questions of *valency*, *proximity*, and *cooperativity among multiple pairs of ligands and receptors*. One may ask, for example, how many ligand-receptor bonds are necessary to "switch on" a specific membrane function? What are the spatial requirements that must be met? How does ligand-receptor cooperativity affect the overall "supramolecular recognition" process (Figure 1)?

Conceptually, *cross-linked polymerized liposomes*, possessing uniform, highly stable and "biomembrane-like" surfaces, represent attractive probes for investigating the above questions.<sup>3</sup> In particular, the ability to control the *spatial availability* of pendant molecules, by adjusting their surface density, and by altering the curvature of the liposomal surface to which they are attached (i.e., by changing the vesicle's size), should allow one to study multivalent binding in a controlled manner. This paper reports the synthesis of a unique class of polymerized liposomes that have been specifically designed for this purpose. Work that will be reported elsewhere will describe the use of such liposomes in defining the supramolecular recognition features of the Arg-Gly-Asp (RGD) moiety toward cell surface receptors.<sup>4,5</sup>

Using methods similar to those previously described, **2** was converted into its corresponding ethanolamine via phospholipase D catalyzed exchange.<sup>6,7</sup> Subsequent treatment with 1.5 equiv of *N*-succinimidyl 3-(2-pyridyldithio)propionate in chloroform and deprotection with 20 equiv of dithiothreitol in methanol afforded **3**.<sup>8</sup>

Surface pressure-area isotherm analysis of monolayers produced from **2** and **3**, at the air-water interface, establish their miscibility.<sup>9</sup> For an ideally miscible or completely immiscible monolayer, the mean area per molecule,  $A_m$  (at a specific surface pressure), is defined by the mole fraction of lipid employed,  $X_1$ , and by the partial molar areas of each lipid ( $A_1$  and  $A_2$ , respectively), according to eq 1. Any deviation from linearity establishes that

$$A_m = X_1A_1 + (1 - X_1)A_2 \quad (1)$$

the pair of surfactants is nonideally miscible. By use of the phase rule of Defay and Crisp, it is also possible to distinguish between

(3) See: Regen, S. L. In *Liposomes: From Biophysics to Therapeutics*; Ostro, M. J., Ed.; Marcel Dekker: New York, 1987; p 73 and references 10–26 cited therein.

(4) The tripeptide sequence RGD has been identified as a key recognition site in certain adhesive promoting proteins: Ruoslahti, E.; Pierschbacher, M. D. *Science* **1987**, *238*, 491 and references cited therein.

(5) Juliano, R. L.; Dodrer, N.; Regen, S. L., unpublished results.

(6) Stefely, J.; Markowitz, M. A.; Regen, S. L. *J. Am. Chem. Soc.* **1988**, *110*, 7463.

(7) Akoka, S.; Meir, C.; Tellier, C.; Belaud, C.; Poignant, S. *Synth. Commun.* **1985**, *15*, 101.

(8) Phospholipids **2** and **3** showed the expected elemental analysis and <sup>1</sup>H NMR (500 MHz), IR, and HRMS spectra.

(9) Gaines, G. L. *Insoluble Monolayers at Liquid-Gas Interfaces*; Wiley-Interscience: New York, 1966; pp 281–286.

(1) Supported by the National Science Foundation (Grant CHE-8703780).

(2) Heim Fellow, 1986–1989.